

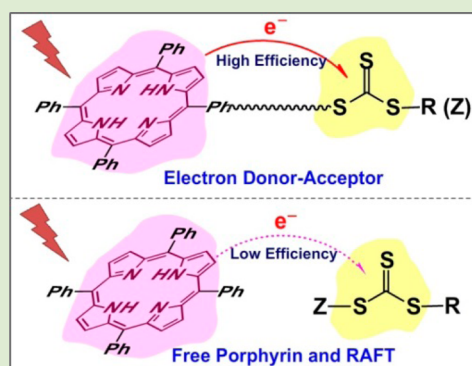
Organic Electron Donor–Acceptor Photoredox Catalysts: Enhanced Catalytic Efficiency toward Controlled Radical Polymerization

Jiangtao Xu,* Sivaprakash Shanmugam, and Cyrille Boyer*

Centre for Advanced Macromolecular Design (CAMD) and Australian Centre for NanoMedicine (ACN), School of Chemical Engineering, UNSW Australia, Sydney, NSW 2052, Australia

S Supporting Information

ABSTRACT: In this study, we designed and synthesized novel organic single electron donor–acceptor molecules containing a free base porphyrin and a thiocarbonylthio group. The porphyrin acts as a light-harvesting antenna and donates an excited electron upon light irradiation to the electron-accepting thiocarbonylthio group. The excited electronic state of the donor–acceptor generates a radical from the thiocarbonylthio compound to activate a living radical polymerization in the presence of monomers. Thus, these donor–acceptor systems play the roles of highly efficient photoredox catalysts and radical initiators. The presence of both donor and acceptor in a single molecule enhanced the electron transfer efficiency in comparison to the donor/acceptor mixture and consequently greatly increased polymerization rates of vinyl monomers under visible light irradiation. The polymerizations mediated by these electron donor–acceptor photoredox catalysts were investigated under green ($\lambda_{\text{max}} = 530 \text{ nm}$, 0.7 mW/cm^2) and red ($\lambda_{\text{max}} = 635 \text{ nm}$, 0.7 mW/cm^2) lights, which exhibited great control over molecular weights, molecular weight distributions, and end-group functionalities.



Fascinated by the ability of natural photosynthetic systems to convert solar energy into chemical energy,¹ the scientific community has recognized the great potential of light-driven reactions (photochemistry) as a powerful and sustainable approach to chemical synthesis.² Photoredox catalysis, harnessing light energy to accelerate chemical reactions via a process of single electron transfer, is one of the most recent and elegant examples. Besides successful implications in organic synthesis,³ photoredox catalysis was initially expanded to conventional photopolymerizations, i.e., uncontrolled free radical polymerization, by Yagci and Lalevee,⁴ and subsequently in living polymerization techniques by Hawker, Fors, Johnson, and ourselves.⁵ The types of photoredox catalysts used to date include transition-metal complexes,^{3e,5f,6} organic dyes,^{5e,7} semiconductors,⁸ and biologically derived compounds.⁵ⁱ

Porphyrins are abundantly occurring in nature and play an important role in harvesting light and catalyzing enzymatic reactions. Therefore, they are popularly employed for artificial dye-sensitizer solar cells⁹ and photocatalysts.¹⁰ Furthermore, they provide an extremely versatile synthetic base for a variety of biomedical and materials applications. The exploration of porphyrin or metalloporphyrin assemblies as building blocks for tailored material properties has grown rapidly during the past several decades.¹¹ Porphyrin has been evaluated in the context of photodynamic therapy since it has extensive light absorption within the visible region.¹²

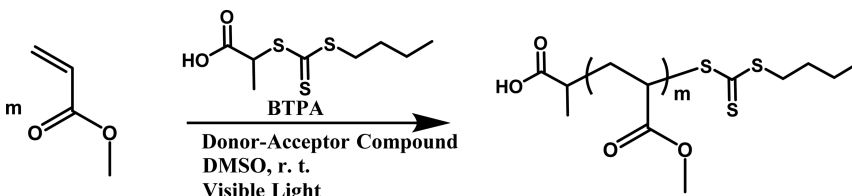
Free base porphyrin has been demonstrated to be both an electron donor and acceptor, depending on the redox potentials of the corresponding acceptor or donor. Our previous research highlighted a visible light mediated living radical polymerization

technique, termed photoinduced electron transfer–reversible addition–fragmentation chain transfer (PET-RAFT),^{5f–j,q} in which a PET process activated a thiocarbonylthio compound to generate radicals. In this process, the thiocarbonylthio compound again plays the role of both initiator and chain transfer agent. Acting as a photoredox catalyst, tetraphenylporphyrin (TPP), one of the most commonly used porphyrins, could regulate photopolymerization of methyl acrylate (MA) in the presence of RAFT agents, such as 2-(*n*-butyltrithiocarbonate)-propionic acid (BTPA) as an electron acceptor to generate radicals (#1 and #6 in Table 1). However, the polymerization rates were really slow even when high catalyst concentrations were applied (500 ppm, data not shown). Thus, here we proposed a concept to use an electron donor–acceptor (EDA) system (Scheme 1) to increase electron transfer efficiency, consequently promoting radical generation and apparent polymerization rates.¹³ In our hypothesis, the electron transfer between TPP and the thiocarbonylthio compound is outer sphere electron transfer, in which both species remain separate and intact before, during, and after the electron transfer event. Upon light irradiation, the electron moves straightforward from donor to acceptor. The distance or collision frequency of the donor and acceptor plays an important role in the electron transfer.¹⁴ In our previous investigations using metal complex porphyrins (chlorophyll a

Received: July 6, 2015

Accepted: August 10, 2015

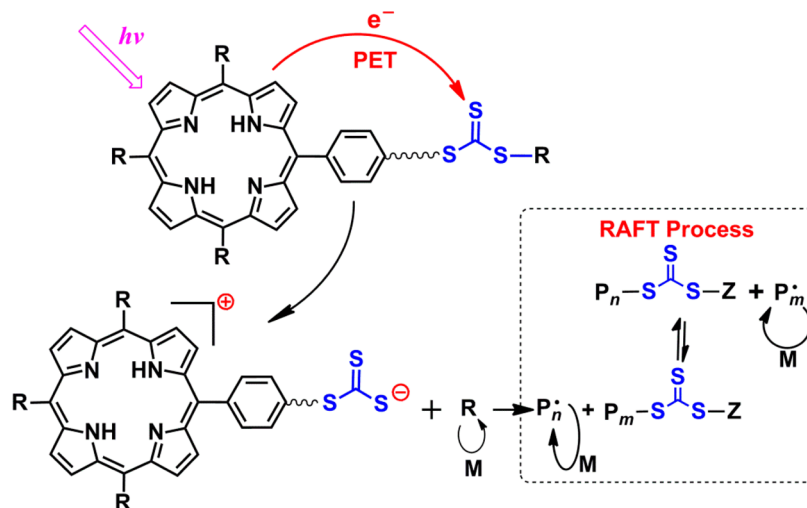
Published: August 17, 2015

Table 1. PET-RAFT Polymerization Mediated by Various Electron Donor–Acceptor (EDA) Compounds under Visible Light^a


no.	photoredox catalyst	light source	RAFT agent	[catalyst]/[M] (ppm)	time (h)	α^b (%)	$M_{n,th}^c$ (g/mol)	$M_{n,GPC}^d$ (g/mol)	M_w/M_n
1	TPP	red	BTPA	100	6	3	-	-	-
2	TPP	red	none	100	6	0	-	-	-
3	TPP-BSTP	red	BTPA	100	6	56	9870	10500	1.07
4	TPP-C ₂ -BSTP	red	BTPA	100	6	23	4200	4670	1.12
5	TPP-C ₂ -BTPA	red	BTPA	100	6	17	-	-	-
6	TPP	green	BTPA	100	6	8	-	-	-
7	TPP	green	none	100	6	0	-	-	-
8	TPP-BSTP	green	BTPA	100	6	63	11070	12110	1.09
9	TPP-C ₂ -BSTP	green	BTPA	100	6	48	8490	9390	1.10
10	TPP-C ₂ -BTPA	green	BTPA	100	6	12	-	-	-

^aExperimental conditions: [MA]:[BTPA]:[EDA] = 200:0.98:0.02; solvent dimethyl sulfoxide (DMSO); light source 5 W red ($\lambda_{max} = 635$ nm, 0.7 mW/cm²) and green ($\lambda_{max} = 530$ nm, 0.7 mW/cm²) LED light. ^bMonomer conversion determined by ¹H NMR spectroscopy. ^cTheoretical molecular weight was calculated using the following equation: $M_{n,th} = [M]_0 / ([BTPA]_0 + [EDA]_0) \times MW^M \times \alpha + MW^{BTPA}$, where $[M]_0$, $[BTPA]_0$, $[EDA]_0$, MW^M , α , and MW^{BTPA} correspond to initial monomer concentration, initial BTPA concentration, electron donor–acceptor compound concentration, molar mass of monomer, conversion determined by ¹H NMR, and molar mass of BTPA. ^dMolecular weight and polydispersity index were determined by GPC analysis (THF as eluent) calibrated to the polystyrene standard.

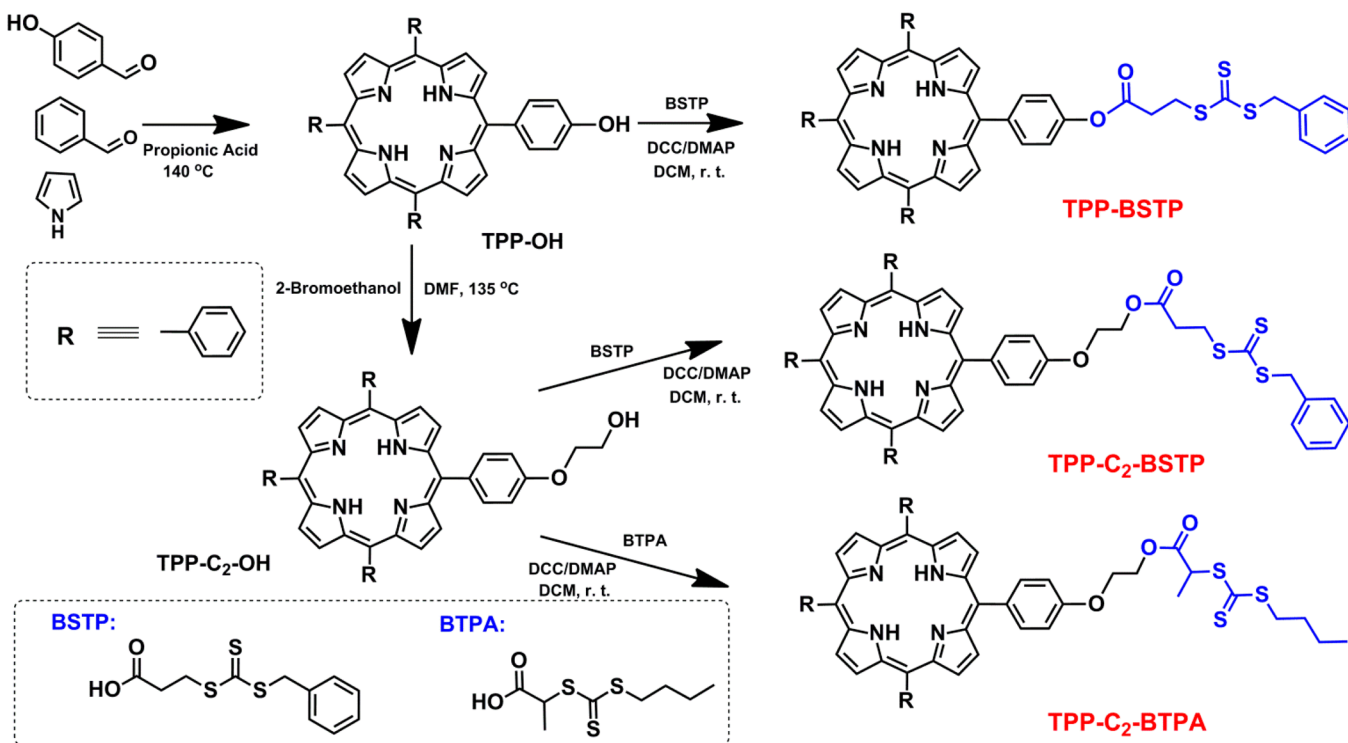
Scheme 1. Designed Electron Donor–Acceptor (EDA) Photoredox Catalyst and Its Plausible Electron Transfer Mechanism



and zinc TPP),^{5i,15} it is different that the transfer of an electron from donor to an acceptor is only fractional, meaning an electron is not completely transferred but results in an electron resonance between the donor and acceptor. This leads to the formation of charge transfer complexes in which the components largely retain their chemical identities.¹⁴ In this contribution, thus we propose to design an EDA system to greatly increase the collision frequency between the electron donor and acceptor because of covalent binding and subsequently promote radical generation from the RAFT moiety. Followed by the RAFT process, controlled polymerization was consequently achieved (Scheme 1). It is worth mentioning that we employed a low energy light source to minimize or suppress the activation of the RAFT agent from plausible energy transfer between porphyrin and the RAFT agent.¹⁶

This concept has been inspired from natural photosynthetic membranes where chlorophyll is acting as the electron donor and stays in close proximity of reaction centers to guarantee an effective electron and energy transfer to activate the Calvin cycle.^{17,18} Such a concept, i.e., EDA systems, is also commonly used in solid solar cell construction, for instance dyes conjugated to C₆₀,¹⁹ carotenoid conjugated to TiO₂,¹⁸ etc. In this contribution, we conjugate an electron donor (porphyrin) and electron acceptor (thiocarbonylthio compounds) via a covalent bond. The efficiency of electron transfer between the donor and acceptor was investigated for the activation of polymerization of acrylate monomers. Therefore, we designed three different EDA compounds shown in Scheme 2.

Two trithiocarbonates (BSTP and BTPA) were selected to covalently link to monofunctionalized TPP using facile chemistry shown in Scheme 2. The resulting electron donor–

Scheme 2. Synthesis of Electron Donor–Acceptor (EDA) Photoredox Catalysts, TPP-BSTP, TPP-C₂-BSTP, and TPP-C₂-BTPA

acceptors differed via the location of the electron donor compound (TPP). BSTP was conjugated to TPP via the Z-group, while BTPA was conjugated via the R-group. The spacers between the donor and acceptor were also varied in length for BSTP as TPP is conjugated in the Z-group of the RAFT agent. The major preparation included the synthesis of electron donor compounds, monohydroxyl-functionalized TPP constituted with two methylene spacers between the hydroxyl and TPP ring (TPP-C₂-OH) and without spacer (TPP-OH). First, TPP-OH was synthesized by refluxing benzaldehyde, 4-hydroxybenzaldehyde, and pyrrole in propionic acid. Although the reaction yield was low (~4%), the purification step was fairly easy by column chromatography. The monofunctional phenolic alcohol, i.e., TPP-OH, was reacted with carboxylic acid terminated BSTP to form the corresponding ester compound with high yield via DCC/DMAP coupling. Therefore, TPP-BSTP was simply prepared by mixing TPP-OH and BSTP in the presence of DCC and DMAP at room temperature. After overnight reaction and purification, 85% yield was obtained. TPP-C₂-OH was synthesized via a nucleophilic substitution by reacting TPP-OH with 2-bromoethanol into DMF at 135 °C to give high yield (86%) product after column purification. After DCC/DMAP coupling between TPP-C₂-OH and BSTP (or BTPA), two products, TPP-C₂-BSTP and TPP-C₂-BTPA, were isolated with high yields. The chemical structures of these EDA compounds were confirmed by ¹H NMR spectroscopy (SI, Figure S1–S4). The UV–vis absorption spectroscopy of these EDA compounds in dimethyl sulfoxide (DMSO) exhibited similar Soret and Q absorption bands at 420 and 500–675 nm, respectively, in comparison with free TPP (SI, Figure S5), which suggests the absence of ground-state complexation between donor and acceptor moieties.

Subsequently, to verify our concept of enhanced catalytic activity in PET-RAFT polymerization where acceptor and donor are conjugated, these EDA compounds were employed

to mediate polymerization of MA in DMSO. The molar ratio of [MA]:[TPP-BSTP] = 10 000:1 (100 ppm catalyst relative to monomer concentration) was applied for polymerization targeting $M_n = 860\,000$ g/mol. After 4 h of red light irradiation, 68% monomer conversion was detected with molecular weight of $M_n = 475\,000$ g/mol and polydispersity of $M_w/M_n = 1.45$. The deviation between experimental and theoretical molecular weights ($M_{n,theo} = 585\,000$ g/mol) was attributed to different polymer standard (polystyrene). Although molecular weight distribution was slightly high due to possible degradation of the RAFT agent from the high ratio of photocatalyst to RAFT agent ([photocatalyst]:[RAFT] = 1:1), the polymerization was proven to be working well. Using identical reaction conditions, control experiments for free TPP and BSTP ([MA]:[TPP]:[BSTP] = 10 000:1:1) gave low monomer conversion (~9%), uncontrolled molecular weight ($M_n = 37\,000$ g/mol), and high polydispersity ($M_w/M_n = 1.7$).

In order to control the molecular weight of final polymers, an external RAFT agent has to be introduced. The formulation of the polymerization reaction mixture was set as [monomer]:[RAFT]:[EDA] = 200:0.98:0.02 (i.e., 100 ppm of TPP relative to monomer concentration). It is worth noting that the EDA compound will also act as a transfer agent as well as an activator for RAFT polymerization. Both RAFT and EDA compounds will generate polymer chains. Although the R groups in TPP-BSTP (and TPP-C₂-BSTP) and BTPA are different, benzyl group vs propionic acid group, the polymerization kinetic behavior will not be affected except the initiation step. As previously mentioned, TPP has a broad absorption band between 490 and 675 nm. Therefore, green LED ($\lambda_{max} = 530$ nm, 0.7 mW/cm²) and red LED ($\lambda_{max} = 635$ nm, 0.7 mW/cm²) light sources were chosen to test MA polymerization. To avoid direct monomer initiation and RAFT agent photolysis, high energy wavelength light sources ($\lambda < 500$ nm) were excluded in this study.¹⁶

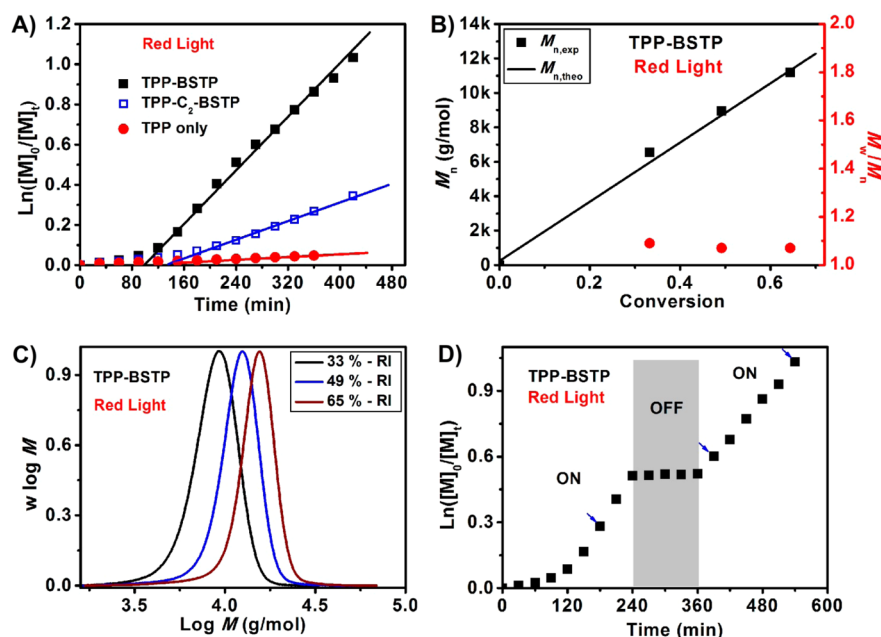


Figure 1. PET-RAFT polymerization of MA mediated by TPP-BSTP, TPP-C₂-BSTP, and TPP as photoredox catalysts in DMSO using BTPA as a chain transfer agent under red light irradiation: (A) $\ln([M]_0/[M]_t)$ vs time of exposure; (B) molecular weights and M_w/M_n vs conversion; (C) molecular weight distributions of PMA at different monomer conversions; (D) “ON–OFF” study for TPP-BSTP. Note: The reactions were performed at room temperature under 5 W red LED light ($\lambda_{\max} = 635$ nm, 0.7 mW/cm²) using $[MA]:[BTPA]:[catalyst] = 200:0.98:0.02$.

For polymerization of MA under red light, monomer conversions for EDA compounds were higher (56%, 23%, and 17% for TPP-BSTP, TPP-C₂-BSTP, and TPP-C₂-BTPA in Table 1, respectively) than that for TPP (3% in Table 1, #1) after 6 h of irradiation. Interestingly, the C₂ spacer in TPP-C₂-BSTP displayed a lower monomer conversion (23%, #4 in Table 1) in comparison with TPP-BSTP (56%, #3 in Table 1). This result was attributed to the distance between acceptor and donor moieties, which limits the electron transfer. It is well-known that the electron and energy transfer reactions in single donor–acceptor molecules are strongly dependent on the donor–acceptor distance.^{13b} In the case of TPP-C₂-BTPA, the donor and acceptor are located at both ends of the polymer chains, while in TPP-BSTP and TPP-C₂-BSTP systems, the donor and acceptor moieties are located at the same end group. In the case of TPP-C₂-BTPA, the monomer insertion separates gradually the donor and acceptor moieties, while polymerization proceeds. As a consequence, the propagation rate decreased (17%, #5 in Table 1).

Polymerization under green light irradiation presented a similar trend (#6–10, Table 1) with those from red light. However, higher monomer conversions were observed under green light (500–550 nm) due to a higher absorption of TPP at 530 nm (SI, Figure S5). After 6 h of light irradiation, 63% and 48% monomer conversions (#8 and #9 in Table 1) were obtained for TPP-BSTP and TPP-C₂-BSTP, respectively. TPP-C₂-BTPA displayed much lower monomer conversion (12%, #10 in Table 1), which demonstrates that the distance between electron donor and acceptor moieties plays a critical role. In the case of TPP-C₂-BSTP, the conversion for green light was higher than that for red light (48% vs 23%) due to the partial photolysis of the RAFT agent.^{16a}

Subsequently, polymerization kinetics were investigated in detail by online Fourier transform near-infrared (FTNIR) spectroscopy for all synthesized EDA compounds under red and green light irradiation. The monomer conversion was

monitored by following the decrease of the vinylic stretching signal of MA at 6250–6100 cm⁻¹.¹⁶ $\ln([M]_0/[M]_t)$ derived from the monomer conversion was plotted against exposure time, as shown in Figure 1A. TPP-BSTP displayed the highest apparent polymerization rate constant, k_p^{app} (red) = 3.12×10^{-3} min⁻¹, with 100 min of induction period, against k_p^{app} (red) = 1.19×10^{-3} min⁻¹ for TPP-C₂-BSTP and k_p^{app} (red) = 0.13×10^{-3} min⁻¹ for TPP, respectively. The induction period could be attributed to slow fragmentation of the RAFT agent similar to traditional RAFT processes.²⁰ Further investigations on this inhibition period will be carried out in the future. Meanwhile, the polymerization mediated by TPP-BSTP suggested living features: linear plot of number-average molecular weight (M_n) versus monomer conversion with low molecular weight distribution (Figure 1B) and symmetrical GPC curves (Figure 1C). In addition, this process has the characteristic feature of temporal control demonstrated by the “ON/OFF” study shown in Figure 1D. The polymerization can be easily stopped and reactivated by switching OFF and ON the light.

The kinetic study for polymerization of MA under green light was identically carried out by online FTNIR spectroscopy (SI, Figure S6). Correspondingly, the apparent polymerization rate constants, k_p^{app} (green) = 3.23×10^{-3} min⁻¹ for TPP-BSTP, k_p^{app} (green) = 2.19×10^{-3} min⁻¹ for TPP-C₂-BSTP, and k_p^{app} (green) = 0.53×10^{-3} min⁻¹ for TPP, indicated faster polymerization under green light than red light, which is in good agreement with the results in Table 1. Furthermore, the induction period was reduced from 100 to 70 min under green light (SI, Figure S6A). For the polymerization mediated by TPP-BSTP, the linear plot of molecular weight (M_n) against monomer conversion (SI, Figure S6B) and symmetrical and monodispersed GPC molecular weight distribution (SI, Figure S6C) reveals a living polymerization behavior.

The versatility of the EDA compounds to other monomers (such as acrylamide) and functionalities was tested under red

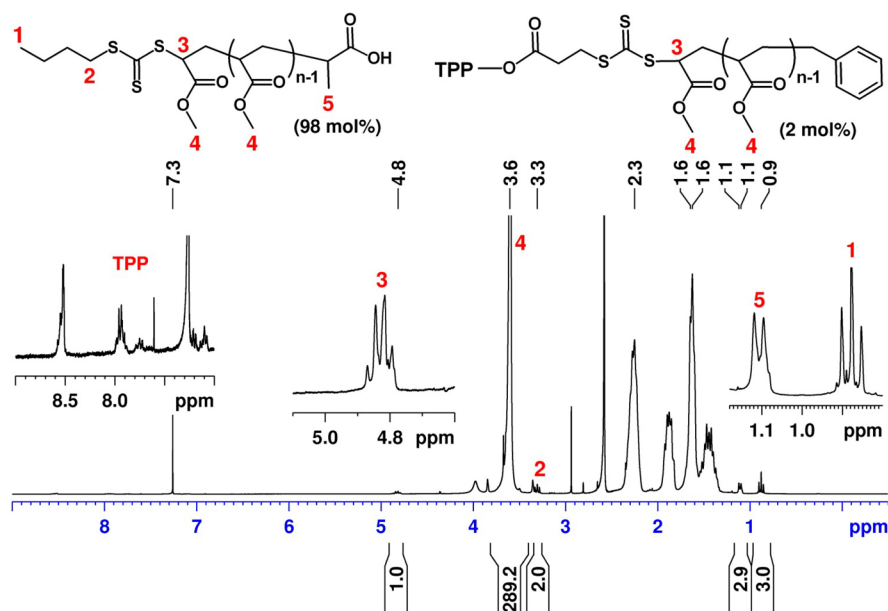


Figure 2. ^1H NMR spectrum for PMA prepared by PET-RAFT polymerization mediated by TPP-BSTP as photoredox catalyst in DMSO using BTPA as the thiocarbonylthio compound under red light irradiation. Note: The reactions were performed at room temperature under 5 W red LED ($\lambda_{\text{max}} = 635 \text{ nm}$) light using $[\text{MA}]:[\text{BTPA}]:[\text{EDA}] = 200:0.98:0.02$, Conversion = 52%, $M_{n,\text{GPC}} = 9180 \text{ g/mol}$, $M_{n,\text{NMR}} = 8500 \text{ g/mol}$, $M_w/M_n = 1.08$.

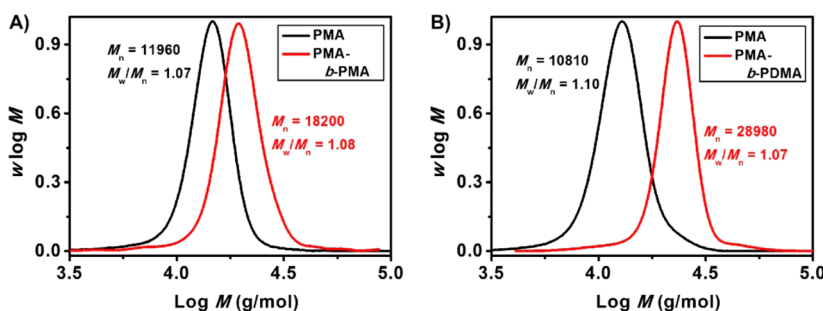


Figure 3. Molecular weight distributions for diblock copolymers PMA-*b*-PMA (A) and PMA-*b*-PDMA (B) prepared by PET-RAFT polymerization using TPP-BSTP as photoredox catalyst in DMSO under red light irradiation.

light irradiation (SI, Table S1). TPP-BSTP was selected as a photoredox catalyst because of its significant catalytic efficiency against others. Reasonable conversions were observed for *N,N*-dimethylacrylamide (DMAA) (57%) and *N*-isopropylacrylamide (NIPAAm) (61%), with low polydispersities (<1.2). Other functionalities (*tert*-butyl, alcohol, tertiary amine, oligo-(ethylene glycol)) were proved to be compatible with this photoredox catalyst because of their living polymerization behavior with controlled molecular weights and low polydispersities.

The final polymer PMA prepared by TPP-BSTP possessed mixed end-groups: minor portion (2 mol % based on the estimated calculation of feeding ratio) with TPP from photoredox catalyst TPP-BSTP and major portion (~ 98 mol %) with BTPA. The minor portion of TPP could be confirmed by the small signal at δ 7.31–9 ppm in the ^1H NMR spectrum (Figure 2) and TPP absorption (Soret band at 420 nm and Q-band from 490–675 nm) in the UV–vis spectrum (SI, Figure S7). The intact UV–vis absorption of resultant PMA at the Soret and Q bands elucidated its integrity of chemical structures. The end-group fidelity could be calculated to be close to 100% by the ratio of integral of signal at δ 4.8 ppm (1 H), 3.3 ppm (2 H), or 0.9 ppm (3 H) to that of the signal at δ 1.1 ppm attributed to CH_3 of the R group in BTPA. The

molecular weight calculated from ^1H NMR ($M_{n,\text{NMR}} = 8500$) matched well with GPC results ($M_{n,\text{GPC}} = 9180 \text{ g/mol}$), indicating excellent control of molecular weight by this technique as well as great livingness of the polymer chain. Chain extension was also investigated to confirm the polymer chain livingness. It is worth noting that the photoredox catalyst was linked to the polymer chain. Therefore, no more extra catalyst was required for chain extensions. Figure 3 showed the molecular weight distributions for macroinitiator PMA and diblock copolymers PMA-*b*-PMA ($[\text{MA}]:[\text{macroinitiator PMA}] = 200:1$) and PMA-*b*-PDMA ($[\text{DMA}]:[\text{macroinitiator PMA}] = 300:1$). The peak clearly shifted to high molecular weights with low polydispersities, suggesting high end-group fidelity and livingness.

In conclusion, a series of novel photoredox catalysts with electron donor–acceptor (EDA) systems were designed and synthesized based on monofunctionalized porphyrin as the electron donor and the thiocarbonylthio group as the electron acceptor. These EDA photoredox catalysts were able to mediate PET-RAFT polymerization with excellent control over molecular weights and molecular weight distributions and enhance electron transfer from donor (porphyrin) to acceptor (thiocarbonylthio group) in comparison to free porphyrin. These findings demonstrated that an efficient PET-RAFT

polymerization required effective interaction or close proximity between the photoredox catalyst and RAFT agent. This study will contribute to facilitating the design and preparation of synthetic materials²¹ or artificial devices for highly efficient light energy conversion. Recently, we reported that ZnTPP is an efficient photoredox catalyst to perform PET-RAFT polymerization.¹⁵ In the following projects, we are planning to incorporate various metals in the TPP ring of these EDA molecules to form metal-doped EDA photoredox catalysts. Our preliminary investigations on ZnTPP-BSTP and ZnTPP-C₂-BTPA containing zinc (see SI, Figures S8 and S9) showed that the inclusion of Zn significantly enhanced the catalytic activity for the polymerization of methyl acrylate. In the case of ZnTPP-BSTP and TPP-BSTP, the monomer conversions obtained with and without Zn were ~73% and 20% after 2 h red light irradiation. The mechanism is currently investigated and will be reported in a further study.

■ ASSOCIATED CONTENT

● Supporting Information

The Supporting Information is available free of charge on the ACS Publications website at DOI: 10.1021/acsmacrolett.5b00460.

Experimental details, UV-vis spectra, NMR spectra, GPC traces (Figures S1–S9) (PDF)

■ AUTHOR INFORMATION

Corresponding Authors

*E-mail: cboyer@unsw.edu.au.

*E-mail: j.xu@unsw.edu.au.

Notes

The authors declare no competing financial interest.

■ ACKNOWLEDGMENTS

C.B. acknowledges Australian Research Council (ARC) for his Future Fellowship (FT120100096) and UNSW (DVCR Prof. Les Field) for funding. The authors thank UNSW Mark Wainwright Analytical Centre.

■ REFERENCES

- (1) Balzani, V.; Credi, A.; Venturi, M. *ChemSusChem* **2008**, *1*, 26–58.
- (2) Ciamician, G. *Science* **1912**, *36*, 385–394.
- (3) (a) Nicewicz, D. A.; MacMillan, D. W. C. *Science* **2008**, *322*, 77–80. (b) Pirnot, M. T.; Rankic, D. A.; Martin, D. B. C.; MacMillan, D. W. C. *Science* **2013**, *339*, 1593–1596. (c) Prier, C. K.; Rankic, D. A.; MacMillan, D. W. C. *Chem. Rev.* **2013**, *113*, 5322–5363. (d) Noble, A.; McCarver, S. J.; MacMillan, D. W. C. *J. Am. Chem. Soc.* **2015**, *137*, 624–627. (e) Narayanan, J. M. R.; Stephenson, C. R. J. *Chem. Soc. Rev.* **2011**, *40*, 102–113. (f) Wallentin, C. J.; Nguyen, J. D.; Finkbeiner, P.; Stephenson, C. R. J. *J. Am. Chem. Soc.* **2012**, *134*, 8875–8884. (g) Devery, J. J.; Stephenson, C. R. J. *Nature* **2015**, *519*, 42–43. (h) Yoon, T. P.; Ischay, M. A.; Du, J. N. *Nat. Chem.* **2010**, *2*, 527–532. (i) Lu, Z.; Yoon, T. P. *Angew. Chem., Int. Ed.* **2012**, *51*, 10329–10332. (j) Schultz, D. M.; Yoon, T. P. *Science* **2014**, *343*, 985–989.
- (4) (a) Lalevee, J.; Blanchard, N.; Tehfe, M. A.; Morlet-Savary, F.; Fouassier, J. P. *Macromolecules* **2010**, *43*, 10191–10195. (b) Lalevee, J.; Dumur, F.; Mayer, C. R.; Gignes, D.; Nasr, G.; Tehfe, M. A.; Telitel, S.; Morlet-Savary, F.; Graff, B.; Fouassier, J. P. *Macromolecules* **2012**, *45*, 4134–4141. (c) Lalevee, J.; Tehfe, M. A.; Dumur, F.; Gignes, D.; Blanchard, N.; Morlet-Savary, F.; Fouassier, J. P. *ACS Macro Lett.* **2012**, *1*, 286–290. (d) Lalevee, J.; Telitel, S.; Xiao, P.; Lepeltier, M.; Dumur, F.; Morlet-Savary, F.; Gignes, D.; Fouassier, J. P. *Beilstein J. Org. Chem.* **2014**, *10*, 863–876. (e) Xiao, P.; Zhang, J.; Dumur, F.; Tehfe, M. A.; Morlet-Savary, F.; Graff, B.; Gignes, D.; Fouassier, J. P.; Dumur, F.; Morlet-Savary, F.; Poly, J.; Lalevee, J. *Macromolecules* **2015**, *48*, 1972–1980. (g) Tasdelen, M. A.; Uygun, M.; Yagci, Y. *Macromol. Chem. Phys.* **2010**, *211*, 2271–2275.
- (5) (a) Fors, B. P.; Hawker, C. J. *Angew. Chem., Int. Ed.* **2012**, *51*, 8850–8853. (b) Fors, B. P.; Poelma, J. E.; Menyo, M. S.; Robb, M. J.; Spokoiny, D. M.; Kramer, J. W.; Waite, J. H.; Hawker, C. J. *J. Am. Chem. Soc.* **2013**, *135*, 14106–14109. (c) Poelma, J. E.; Fors, B. P.; Meyers, G. F.; Kramer, J. W.; Hawker, C. J. *Angew. Chem., Int. Ed.* **2013**, *52*, 6844–6848. (d) Treat, N. J.; Fors, B. P.; Kramer, J. W.; Christianson, M.; Chiu, C. Y.; de Alaniz, J. R.; Hawker, C. J. *ACS Macro Lett.* **2014**, *3*, 580–584. (e) Treat, N. J.; Sprafke, H.; Kramer, J. W.; Clark, P. G.; Barton, B. E.; de Alaniz, J. R.; Fors, B. P.; Hawker, C. J. *J. Am. Chem. Soc.* **2014**, *136*, 16096–16101. (f) Xu, J. T.; Jung, K.; Atme, A.; Shanmugam, S.; Boyer, C. *J. Am. Chem. Soc.* **2014**, *136*, 5508–5519. (g) Xu, J. T.; Jung, K.; Boyer, C. *Macromolecules* **2014**, *47*, 4217–4229. (h) Xu, J. T.; Jung, K.; Corrigan, N. A.; Boyer, C. *Chem. Sci.* **2014**, *5*, 3568–3575. (i) Shanmugam, S.; Xu, J. T.; Boyer, C. *Chem. Sci.* **2015**, *6*, 1341–1349. (j) Shanmugam, S.; Xu, J. T.; Boyer, C. *Macromolecules* **2014**, *47*, 4930–4942. (k) Ciftci, M.; Tasdelen, M. A.; Yagci, Y. *Polym. Chem.* **2014**, *5*, 600–606. (l) Dadashi-Silab, S.; Tasdelen, M. A.; Yagci, Y. *J. Polym. Sci., Part A: Polym. Chem.* **2014**, *52*, 2878–2888. (m) Anastasaki, A.; Nikolaou, V.; Zhang, Q.; Burns, J.; Samanta, S. R.; Waldron, C.; Haddleton, A. J.; McHale, R.; Fox, D.; Percec, V.; Wilson, P.; Haddleton, D. M. *J. Am. Chem. Soc.* **2014**, *136*, 1141–1149. (n) Anastasaki, A.; Nikolaou, V.; Brandford-Adams, F.; Nurumbetov, G.; Zhang, Q.; Clarkson, G. J.; Fox, D. J.; Wilson, P.; Kempe, K.; Haddleton, D. M. *Chem. Commun.* **2015**, *51*, 5626–5629. (o) Anastasaki, A.; Nikolaou, V.; McCaul, N. W.; Simula, A.; Godfrey, J.; Waldron, C.; Wilson, P.; Kempe, K.; Haddleton, D. M. *Macromolecules* **2015**, *48*, 1404–1411. (p) Chen, M.; MacLeod, M. J.; Johnson, J. A. *ACS Macro Lett.* **2015**, *4*, 566–569. (q) Shanmugam, S.; Boyer, C. *J. Am. Chem. Soc.* **2015**, DOI: 10.1021/jacs.5b05903.
- (6) Xu, J. T.; Atme, A.; Martins, A. F. M.; Jung, K.; Boyer, C. *Polym. Chem.* **2014**, *5*, 3321–3325.
- (7) Xu, J.; Shanmugam, S.; Duong, H. T.; Boyer, C. *Polym. Chem.* **2015**, *6*, 5615–5624.
- (8) (a) Kiskan, B.; Zhang, J. S.; Wang, X. C.; Antonietti, M.; Yagci, Y. *ACS Macro Lett.* **2012**, *1*, 546–549. (b) Sun, J. H.; Zhang, J. S.; Zhang, M. W.; Antonietti, M.; Fu, X. Z.; Wang, X. C. *Nat. Commun.* **2012**, *1139*. (c) Zheng, Y.; Lin, L. H.; Ye, X. J.; Guo, F. S.; Wang, X. C. *Angew. Chem., Int. Ed.* **2014**, *53*, 11926–11930. (d) Ravelli, D.; Protti, S.; Albini, A. *Molecules* **2015**, *20*, 1527–1542.
- (9) (a) Kwok, E. C. H.; Chan, M. Y.; Wong, K. M. C.; Yam, V. W. W. *Chem. - Eur. J.* **2014**, *20*, 3142–3153. (b) Lee, S.; Sarker, A. K.; Hong, J. D. *Bull. Korean Chem. Soc.* **2014**, *35*, 3052–3058. (c) Pelleja, L.; Kumar, C. V.; Clifford, J. N.; Palomares, E. *J. Phys. Chem. C* **2014**, *118*, 16504–16509. (d) Wang, Y. Q.; Chen, B.; Wu, W. J.; Li, X.; Zhu, H. H.; Tian, H.; Xie, Y. S. *Angew. Chem., Int. Ed.* **2014**, *53*, 10779–10783.
- (10) (a) Shiragami, T.; Matsumoto, J.; Inoue, H.; Yasuda, M. *J. Photochem. Photobiol., C* **2005**, *6*, 227–248. (b) Silva, M.; Azenha, M. E.; Pereira, M. M.; Burrows, H. D.; Sarakha, M.; Forano, C.; Ribeiro, M. F.; Fernandes, A. *Appl. Catal., B* **2010**, *100*, 1–9.
- (11) (a) Feng, D. W.; Gu, Z. Y.; Li, J. R.; Jiang, H. L.; Wei, Z. W.; Zhou, H. C. *Angew. Chem., Int. Ed.* **2012**, *51*, 10307–10310. (b) Feng, D. W.; Chung, W. C.; Wei, Z. W.; Gu, Z. Y.; Jiang, H. L.; Chen, Y. P.; Darensbourg, D. J.; Zhou, H. C. *J. Am. Chem. Soc.* **2013**, *135*, 17105–17110. (c) Priola, S. A.; Raines, A.; Caughey, W. S. *Science* **2000**, *287*, 1503–1506. (d) Yella, A.; Lee, H. W.; Tsao, H. N.; Yi, C. Y.; Chandiran, A. K. *Science* **2011**, *334*, 1203–1203.
- (12) (a) Ethirajan, M.; Chen, Y.; Joshi, P.; Pandey, R. K. *Chem. Soc. Rev.* **2011**, *40*, 340–362. (b) O'Connor, A. E.; Gallagher, W. M.; Byrne, A. T. *Photochem. Photobiol.* **2009**, *85*, 1053–1074.
- (13) (a) Kawamura, K.; Amemiya, T.; Nakai, Y.; Takashima, M. *J. Photopolym. Sci. Technol.* **2009**, *22*, 591–596. (b) Yonemoto, E. H.; Saube, G. B.; Schmehl, R. H.; Hubig, S. M.; Riley, R. L.; Iverson, B. L.; Mallouk, T. E. *J. Am. Chem. Soc.* **1994**, *116*, 4786–4795.

(14) (a) Mulliken, R. S. *J. Am. Chem. Soc.* **1952**, *74*, 811–824. (b) Castner, E. W.; Kennedy, D.; Cave, R. J. *J. Phys. Chem. A* **2000**, *104*, 2869–2885.

(15) Shanmugam, S.; Xu, J.; Boyer, C. *J. Am. Chem. Soc.* **2015**, *137*, 9174–9185.

(16) (a) Xu, J.; Shanmugam, S.; Corrigan, N. A.; Boyer, C. In *Controlled Radical Polymerization: Mechanisms*; American Chemical Society: Washington DC, 2015; Vol. 1187, pp 247–267. (b) McKenzie, T. G.; Fu, Q.; Wong, E. H. H.; Dunstan, D. E.; Qiao, G. G. *Macromolecules* **2015**, *48*, 3864–3872.

(17) Imahori, H. *Org. Biomol. Chem.* **2004**, *2*, 1425–1433.

(18) Pan, J.; Xu, Y.; Sun, L.; Sundström, V.; Polívka, T. *J. Am. Chem. Soc.* **2004**, *126*, 3066–3067.

(19) (a) Wróbel, D.; Graja, A. *Coord. Chem. Rev.* **2011**, *255*, 2555–2577. (b) Wicht, G.; Bücheler, S.; Dietrich, M.; Jäger, T.; Nüesch, F.; Offermans, T.; Tisserant, J.-N.; Wang, L.; Zhang, H.; Hany, R. *Sol. Energy Mater. Sol. Cells* **2013**, *117*, 585–591.

(20) Rizzardo, E.; Chen, M.; Chong, B.; Moad, G.; Skidmore, M.; Thang, S. H. *Macromol. Symp.* **2007**, *248*, 104–116.

(21) (a) Liu, G.; Hu, J.; Zhang, G.; Liu, S. *Bioconjugate Chem.* **2015**, *26*, 1328–1338. (b) Hu, X.; Hu, J.; Tian, J.; Ge, Z.; Zhang, G.; Luo, K.; Liu, S. *J. Am. Chem. Soc.* **2013**, *135*, 17617–17629. (c) Hu, X.; Liu, G.; Li, Y.; Wang, X.; Liu, S. *J. Am. Chem. Soc.* **2015**, *137*, 362–368.